Original Article

HER2 transmembrane domain mutation: comprehensive characteristics and real-world evidence of treatment response in Chinese lung adenocarcinoma

Ziqi Jia[1,2#], Jiahua Xing[3#], Ji Li[4#], Weiwei Wang[1], Yadong Wang[1], Yang Song[1], Xiaoying Yang[1,2], Jianchao Xue[1], Junyi Ye[5], Bing Li[5], Han Han-Zhang[6], Jiaxing Zhao[6], Xiaochun Zhang[7], Feng Peng[8], Fengxia Chen[9], Xueqin Chen[10], Yan Lu[11], Shenpeng Ying[12], Dongping Wu[13], Xinwei Zhang[14], Caixia Ma[15], Lipeng Lai[15], Songling Ma[15], Dianjing Liang[16], Peng Liu[17], Xiaoguang Li[18], Naixin Liang[1], Shanqing Li[1]

[1]Department of Thoracic Surgery, Peking Union Medical College Hospital, Peking Union Medical College and Chinese Academy of Medical Sciences, Beijing, China; [2] Eight-Year MD Program, Peking Union Medical College and Chinese Academy of Medical Sciences, Beijing, China; [3]School of Medicine, Nankai University, Tianjin, China; [4]Department of Pathology, Peking Union Medical College Hospital, Chinese Academy of Medical Sciences, Beijing, China; [5]Department of Biostatistics, Burning Rock Biotech Co. Ltd., Guangzhou, China; [6]Department of Medicine, Burning Rock Biotech Co. Ltd., Guangzhou, China; [7]Precision Medicine Center of Cancer, The Affiliated Hospital of Qingdao University, Qingdao, China; [8]Department of Thoracic Cancer, Cancer Center, West China Hospital, S.C.U., Chengdu, China; [9]Department of Thoracic Surgery, Hainan General Hospital, Haikou, China; [10]Department of Oncology, Affiliated Hangzhou First People's Hospital, Zhejiang University School of Medicine, Hangzhou, China; [11]Department of Oncology, Yueyang Hospital of Integrated Traditional Chinese and Western Medicine, Shanghai University of Traditional Chinese Medicine, Shanghai, China; [12]Department of Radiotherapy, Taizhou Central Hospital, Affiliated Hospital of Taizhou University, Taizhou, China; [13]Department of Radiation Oncology, Shaoxing People's Hospital, Shaoxing Hospital of Zhejiang University, Shaoxing, China; [14]Department of Biotherapy, Cancer Institute and Hospital, Tianjin Medical University, Tianjin, China; [15]XtalPi, XtalPi AI Research Center, Beijing, China; [16]Institute of Physics, Humboldt University of Berlin, Berlin, Germany; [17]Medical Research Center, Central Laboratory, Peking Union Medical College Hospital, Chinese Academy of Medical Sciences, Beijing, China; [18]Minimally Invasive Tumor Therapies Center, Beijing Hospital, National Center of Gerontology; Institute of Geriatric Medicine, Chinese Academy of Medical Sciences, Beijing, China

Contributions: (I) Conception and design: Z Jia, J Zhao, N Liang, S Li; (II) Administrative support: N Liang, S Li; (III) Provision of study materials or patients: X Zhang, F Peng, F Chen, X Chen, Y Lu, S Ying, D Wu, X Zhang; (IV) Collection and assembly of data: Z Jia, J Xing, W Wang, Y Wang, X Yang, Y Song, J Xue; (V) Data analysis and interpretation: Z Jia, J Xing, J Ye, B Li, H Zhang, J Zhao, D Liang; (VI) Manuscript writing: All authors; (VII) Final approval of manuscript: All authors.

[#]These authors contributed equally to this work.

Correspondence to: Naixin Liang, MD. Department of Thoracic Surgery, Peking Union Medical College Hospital, Peking Union Medical College and Chinese Academy of Medical Sciences, Beijing 100730, China. Email: pumchnelson@163.com.

Background: *HER2* transmembrane domain (TMD) mutation has been reported as a rare driver mutation associated with advanced stage disease and a poor prognosis in patients with lung adenocarcinoma (LUAD). We aimed to comprehensively profile the genetic landscape and treatment response information of *HER2* TMD-mutant LUAD.

Methods: An in-house database of 7,812 LUAD patients was screened for mutation prevalence. A multi-center cohort of 16 *HER2* V659E-mutant patients and an external cohort of 38 *HER2*-mutant patients from cBioPortal with overall survival (OS) data were analyzed. Eight patients from the in-house cohort were included in the real-world study of treatment response. Molecular docking simulation and binding affinity prediction were performed.

Results: In Chinese LUAD, the prevalence of *HER2* TMD mutation was 0.18% (14/7,812), and 0.14% (11/7,812) for the *HER2* V659E mutation. The most recurrent co-alteration was *TP53* mutation (n=4, 25%) and *HER2* amplification (n=2, 12.5%). TMD-mutant patients were diagnosed at more advance stages (P<0.001) and had poorer OS (median OS 10.0 *vs.* 61.6 months, HR =7.9, 95% CI: 1.0–61.0, P<0.001) than non-TMD mutations. The overall response rate of targeted therapy, chemo-based therapy, and immunotherapy was 57.1%, 22.2%, and 0%, respectively. We postulated to challenge the resistance

of tyrosine kinase inhibitor (TKI) with another with stronger binding energy to HER2 and supported the conclusion with a successful case. Additionally, we demonstrated a three-month response to the off-label use of pyrotinib in fifth-line therapy.

Conclusions: Comapred with non-TMD mtuations, *HER2* TMD mutation is a rare driver mutation with poorer prognosis in LUAD. Targeted therapy is the dominant choice for patients harboring this targetable mutation and longer OS could possibly be achieved through rechallenge with TKI of stronger binding affinity. Response to fifth-line pyrotinib was observed.

Keywords: *HER2* mutation; lung adenocarcinoma (LUAD); prognosis; treatment response; pyrotinib

Submitted Jan 08, 2021. Accepted for publication Mar 25, 2021.
doi: 10.21037/tlcr-21-107
View this article at: http://dx.doi.org/10.21037/tlcr-21-107

Introduction

The comprehensive management of non-small cell lung cancer (NSCLC) has been revolutionized, switching from a one-treatment-fits-all approach to personalized medicine (1). With the advancements in next-generation sequencing (NGS), numerous driver mutations have been revealed and treatments have attained higher precision (2). Tumor NGS reports are detailed into specific alterations and mutation loci, as mutations at different loci of the same gene might lead to different treatment responses (3). Mutations at rare loci acting as driver mutations have also been found.

Erb-b2 receptor tyrosine kinase 2 (*HER2/ERBB2*) is one of the driver genes identified that are susceptible to targeted treatments (4). *HER2* alteration is usually seen as amplification (2–23%) and/or overexpression (11–32%) in lung adenocarcinoma (LUAD), but rarely as mutations (1.6–4%) (5-7). *HER2* mutation is a distinct therapeutic target and a poor prognosis predictor (8-10). Most of the *HER2*-mutant NSCLCs are adenocarcinomas and occur in female never-smokers (8,11,12). Overall survival of *HER2*-mutant NSCLCs is 28.4 months (8) and ranges from 19.2 to 22.8 months among those diagnosed at stage IV (11,13). The gene product of *HER2* is a membrane protein by the same name, which is a receptor tyrosine kinase that forms homodimers or heterodimers to activate downstream pathways (14) and has a transmembrane domain (TMD) where intramolecular interactions occur and lead to dimerization and activation (14). In LUAD, most *HER2* mutations occur in the kinase domain (KD, 2–4%), but rarely in the TMD (0.07–0.20%) (8,15-19). Moreover, activating TMD mutations most frequently affect residues V659 and G660 in exon 17 (20-23).

Most HER2-targeting agents such as trastuzmab did not result in comparable efficacy in NSCLC harboring *HER2* exon 20 mutations as they did in HER2-positive breast cancer. A mechanistic explanation is yet to be established but may implicate intratumoral heterogeneity and lower *HER2* expression in *HER2*-mutant NSCLC compared with in *HER2*-amplified breast cancer (24). Theraies for *HER2*-mutant NSCLC is under active development, among which the most promising include reversible or irreversible anti-HER2 TKIs and antibody-drug conjugates (ADCs) that target HER2 alone or along with EGFR (25). Patients harboring a *HER2* TMD mutations were reported to respond to HER2 tyrosine kinase inhibitor (TKI), lapatinib, and afatinib in case reports (15,26); and to the antibody-drug conjugate, ado-trastuzumab emtansine (TDM-1) in a basket trial (9). Due to their low prevalence, it remains to be determined whether TMD mutations would result in a comparable response to targeted therapy as *HER2* KD mutations.

Herein, we demonstrated the comprehensive characteristics and prognosis of the *HER2* TMD-mutant population and illustrated the real-world evidence (RWE) of treatment response from the largest reported LUAD cohort that harbors *HER2* V659E mutation. To enrich the limited clinical data on how to overcome resistance to targeted therapy, we postulated to challenge the resistance of former-line TKI with TKI that has stronger binding energy to the ATP-pocket of HER2 KD mutants. Additionally, we demonstrated a three-month response to the off-label use of pyrotinib in fifth-line therapy. We present the following article in accordance with the MDAR reporting checklist (available at http://dx.doi.org/10.21037/tlcr-21-107).

Methods

Database, sample collection, and NGS

We screened the genomic profiles of samples from

7,812 Chinese LUAD patients in the Burning Rock LAVA Open-access Database, profiled between Jan 2014 and July 2019. As an external cohort, a total of 4,587 samples of 4,185 patients was selected from The Cancer Genome Atlas (TCGA) and other studies (27-37) through the open platform cBioPortal for Cancer Genomics (38,39). After deduplication, a total of 2,966 patients with 3,480 samples were included. In brief, 38 *HER2*-mutant patients with overall survival (OS) were deduplicated and included in the final analysis. Protocols of sample collection, DNA extraction, and plasma cell-free DNA preparation were as previously described (40). Captured-based targeted NGS using various panels, including panels with eight, 168, or 520 cancer-related genes (Burning Rock Biotech, Guangzhou, China) were performed according to protocols as previously described (41). The panel gene lists are shown in Tables S1-S3. TMD is defined as 27 amino acids (Ala648 to Leu674), and KD is defined as 274 amino acids (Ile714 to Val987) (42).

Clinical characteristics and response assessment

Patient characteristics, treatments, and outcomes were obtained from the LAVA database with the permission of patients and their physicians in-charge. Patients were followed from the date of diagnosis until death or the last available follow-up. Response to therapy was measured using RECIST v1.1 criteria and OS was calculated from the date of the initiation of treatment until the day of last follow-up or death. All procedures performed in studies involving human participants were in accordance with the Helsinki Declaration (as revised in 2013). The study was conducted under the approval of the Ethics Committee of Peking Union Medical College Hospital (ZS-1329). Written informed consent was obtained from each patient.

Computational methods of simulation and energy analysis of lapatinib, afatinib, and pyrotinib in HER2 KD binding

AutoDock 4.2 (43) was used for molecular docking simulations of lapatinib, afatinib, and pyrotinib and predicting binding affinity with the HER2 KD (PDB code:3RCD). The Lamarckian genetic algorithm (LGA) (44) was used to optimize the binding conformations of compounds. The structure of the lowest predicted binding free energy in the most popular cluster of each compound was selected as the initial conformation for the following molecular dynamic (MD) simulation. MD simulations were implemented by AMBER18 (45). The potentials for protein and ligands in each complex were generated based on AMBER03 (parm03) forcefield (46), and general amber forcefield (gaff) (47), respectively. Partial atomic charges were assigned using the AM1-BCC charge method (48,49) within the ANTECHAMBER in AMBERTools12 (50). The compound was neutralized with the counterions of Cl^- and the whole system was immersed in a truncated octahedron's box of TIP3PBOX water (51). The periodic boundary is 12 Å from any solute atoms. The binding free energy was evaluated by the MMGBSA method, which is based on the following equation (52):

$$\Delta G_{bind} = G_{complex} - G_{protein} - G_{ligand} = \Delta E_{MM} + \Delta G_{GB} + \Delta G_{SA} - T\Delta S = \Delta E_{vdw} + \Delta E_{ele} + \Delta G_{GB} + \Delta G_{SA} - T\Delta S \quad [1]$$

where ΔE_{MM} is the molecular mechanics interaction energy between the protein and the ligand, which is comprised of two parts: the electrostatic (ΔE_{ele}) and the van der Waals energies (ΔE_{vdW}). Further, ΔG_{GB} and ΔG_{SA} are the polar and nonpolar contributions of the desolvation free energy upon the construction of the protein-substrate complex. The 200 snapshots taken from the last 6.0 ns MD simulation trajectories of the complex were used to calculate the protein-substrate binding free energy, which was accomplished by the MMPBSA.py program in AmberTools18 (53).

Statistical analysis

Clinical characteristics between the group of *HER2* TMD-mutant patients with OS data and the group of *HER2* non-TMD mutation with OS data were performed with Student *t*-test if the characteristic was a continuous variable; with Chi-square test if the characteristic was a binary variable; and with non-parametric Mann-Whitney test if the characteristic was a ranked variable. Kaplan Meier curves for OS of the two above-mentioned groups were plotted. Pairwise comparisons using log-rank test were performed and the P value was adjusted using the Benjamini-Hochberg method. Cox regression model was used in the univariate and multivariate analysis. All the above-mentioned statistical analyses were conducted in R Studio using Package survminer (v0.4.7; http://cran.r-project.org/web/packages/survminer/index.html), ggplot2 (54), and survival (55).

Results

Comprehensive characteristics of the HER2 TMD mutated LUAD

We analyzed the NGS data of 7,812 LUAD patients and

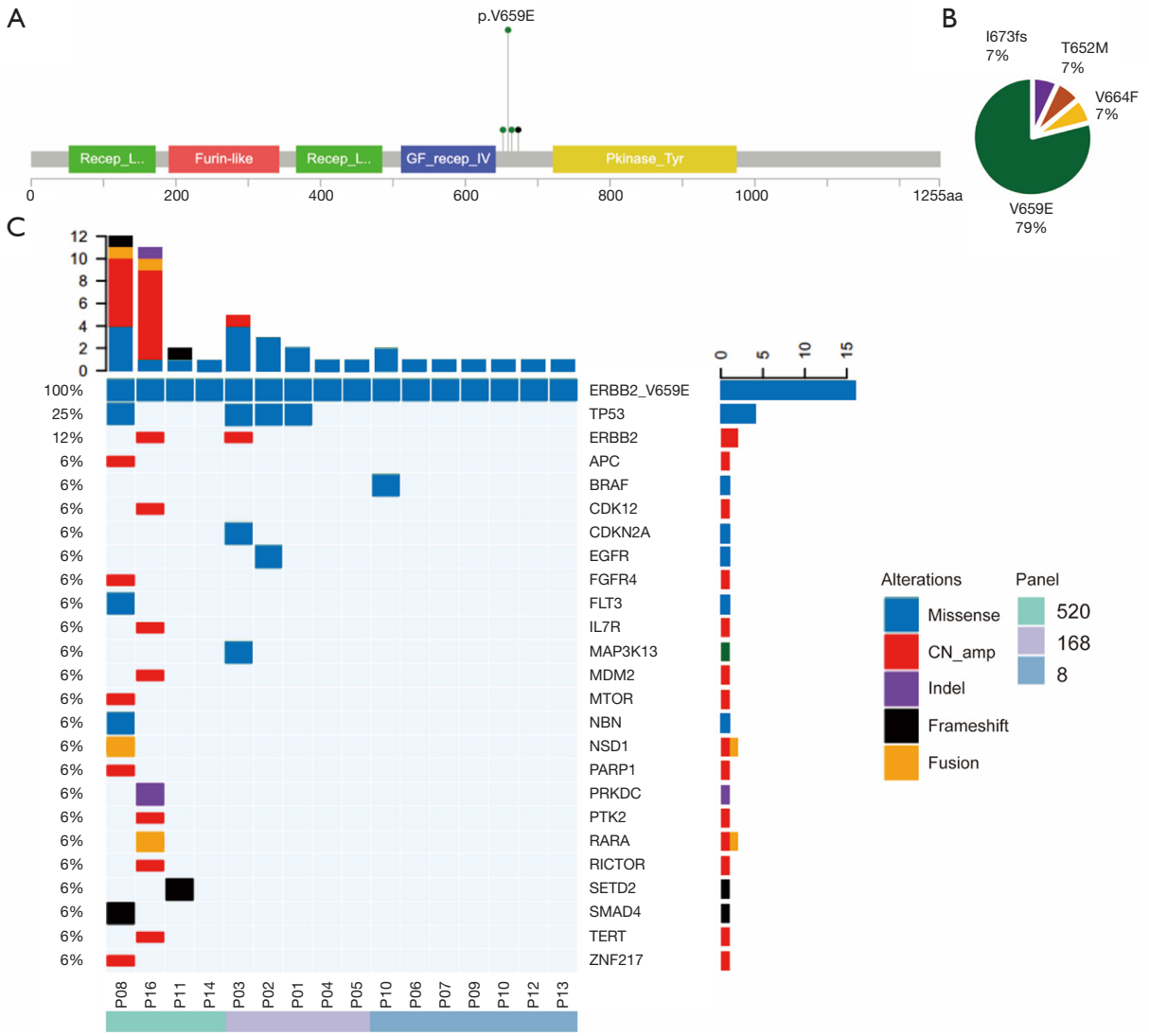

Figure 1 Molecular characteristics of *HER2* TMD mutations. (A) An overview of the *HER2* TMD mutation region in the LAVA database. The mutation region is referred to the Pfam database. (B) Constitution of *HER2* TMD mutation cohort in the LAVA database. (C) Oncoprint of concurrent mutations of oncogenes and tumor suppressor genes in patients with *HER2* TMD mutations. Four patients used 520 cancer-related gene panel, five used 168 cancer-related gene panel, and seven used 8 cancer-related gene panel. Right Y axis shows gene names of the concurrent gene mutation and left Y axis shows the percentage of patients harboring such concurrent mutation. TMD, transmembrane domain.

identified 14 (0.18%) with a *HER2* TMD mutation. These TMD mutations covered four amino acids among the 27 amino acids of the *HER2* TM domain (*Figure 1A,B*). The most mutations occurred at codon 659, which were mostly V659E mutation (11/7,812, 0.14%). Seven patients from the external cohort of 2,966 NSCLC patients harbored a *HER2* TMD mutation (0.24%) and three of these harbored a *HER2* V659E mutation (0.10%). A retrospective search in medical records from cooperating medical centers assembled a cohort of 16 *HER2* V659E-mutant patients (*Table 1*), and detailed characteristics of the patients are shown in Table S4. Five of these patients were not included in the formal analysis, and eight did not have follow-up information. In this cohort, the tumors of all patients were LUAD and harbored a dinucleotide missense mutation, including 10 TT→AA and 6 TT→AG (c.1976_1977). There were equal numbers of males and females (n=8 for each), and 68.75% were non-smokers (n=11). Most of the tumors

Table 1 Clinicopathological and genetic characteristics of cohorts harboring *HER2* TMD or non-TMD mutations

Variable	*HER2* TMD mutation[1] (n=16)	*HER2* TMD mutation with OS data[2] (n=10)	*HER2* non-TMD mutation with OS data[3] (n=36)	P value
Age, mean (SD)	62.75 (10.50)	64.40 (8.58)	64.00 (9.98)	0.93
Sex (%)				0.10
Female	8 (50.00)	2 (20.00)	20 (66.67)	
Male	8 (50.00)	8 (80.00)	16 (53.33)	
Stage (%)				<0.001
I	3 (18.75)	0 (0.00)	24 (80.00)	
II	0 (0.00)	0 (0.00)	6 (20.00)	
III	0 (0.00)	0 (0.00)	5 (16.67)	
IV	13 (81.25)	10 (100.00)	1 (3.33)	
Pathology (%)				0.24
LUAD	16 (100.00)	10 (100.00)	27 (90.00)	
LUSC	0 (0.00)	0 (0.00)	9 (30.00)	
Smoker (%)				0.13
Yes	11 (68.75)	3 (30.00)	25 (83.33)	
No	5 (31.25)	7 (70.00)	7 (23.33)	
Unknown	0 (0.00)	0 (0.00)	4 (13.33)	
HER2 alteration				<0.001
TMD	16 (100.00)	10 (100.00)	0 (0.00)	
V659E mutation				
c.1976_1977delTTinsAA	1 (6.25)	1 (10.00)	–	
c.1976_1977delinsAG	6 (37.50)	1 (10.00)	–	
c.1976_1977inv	3 (18.75)	2 (20.00)	–	
c.1976_1978inv	3 (18.75)	1 (10.00)	–	
c.1976_1979inv	2 (12.50)	2 (20.00)	–	
c.1976_1980inv	1 (6.25)	1 (10.00)	–	
non-V659E mutation	0 (0.00)	2 (20.00)	–	
KD	0 (0.00)	0 (0.00)	14 (46.67)	
Others	0 (0.00)	0 (0.00)	22 (73.33)	

[1], features of the retrospectively assembled cohort of 16 patients, whose genetic features were analysed. [2], features of the patients of the retrospective cohort and cBioPortal database who harbored a *HER2* TMD mutation and had overall survival (OS) data. [3], features of the patients from cBioPortal database who harbored a *HER2* non-TMD mutation and had overall survival (OS) data. TMD, transmembrane domain; OS, overall survival; SD, standard deviation; LUAD, lung adenocarcinoma; LUSC, lung squamous carcinoma; KD, kinase domain.

harboring *HER2* V659E were diagnosed at an advanced stage (stage III–IV, n=13/16, 81.25%). Among the 16 concomitant genetic alterations (*Figure 1C*), *TP53* was the most frequently mutated gene (n=4, 25.0%) followed by *HER2* amplification (n=2, 12.5%), *NSD1* (n=2, 12.5%) and *RARA* (n=2, 12.5%). The sequencing results of patient 02 and 10 suggested that *HER2* V659E could coexist with the driver mutations *EGFR* (p.T783I) and *BRAF* (p.I659M), though not at their

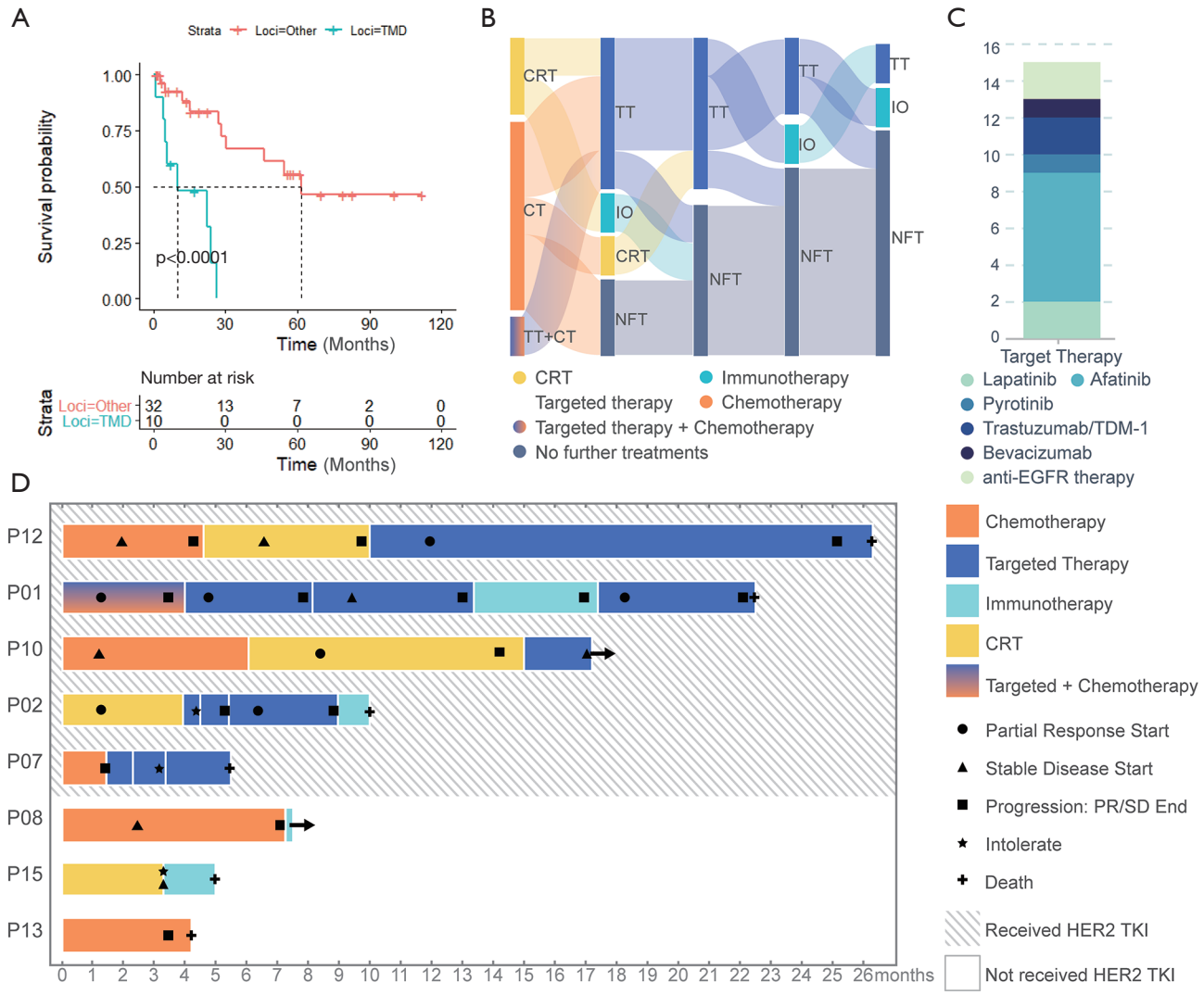

Figure 2 Overall survival and real-world treatment profile. (A) Overall survival in patients from *HER2* TMD and non-TMD mutation cohorts. Log-rank test: P<0.0001. (B) Sankey diagram of treatment regimen of patients with *HER2* TMD mutations. (C) Targeted therapy used in the treatment regimen of patients with *HER2* TMD mutations. (D) Swimmers plot of time on treatment demonstrating PFS to each line of therapy and overall survival. Each bar represents one subject in the study. TMD, transmembrane domain; CRT, chemoradiotherapy; CT, chemotherapy; TT, targeted therapy; IO, immunotherapy; NFT, no further treatments; TKI, tyrosine kinase inhibitor.

hotspots. The eight patients from the in-house cohort with OS information together with two patients from the external cohort harboring *HER2* TMD mutations and with available OS were assembled into a cohort for further survival analysis. Thirty-six patients from the external cohort harboring *HER2* non-TMD mutation were also analyzed as a comparative cohort. These two cohorts were significantly different in the stage of diagnosis (P<0.001) but were comparable from other perspectives.

Real-world evidence of treatments for HER2 V659E patients and responses

Follow-up treatment information was available for eight *HER2* V659E-mutant patients from the in-house cohort, and OS data were available for all 46 patients harboring *HER2* mutations from both in-house and external cohorts. The Kaplan-Meier curves of patients from *HER2* TMD mutation and non-TMD mutation cohorts are shown in *Figure 2A*. The

Table 2 Multivariate survival analysis using Cox regression model in patients with *HER2* TMD or non-TMD mutation

Variables	Univariate		Multivariate	
	HR (95% CI)	P value	HR (95% CI)	P value
Age	0.97 (0.93–1)	0.24	–	–
Gender (male *vs.* female)	1 (0.4–2.5)	0.99	–	–
Pathology (LUSD *vs.* LUAD)	1.8 (0.68–4.9)	0.23	–	–
Smoker (no *vs.* yes)	1.2 (0.44–3.2)	0.73	–	–
Stage	1.9 (1.3–3)	0.0021	1.2 (0.61–2.5)	0.47
HER2 (TMD *vs.* others)	9.3 (2.7–32)	0.00039	7.9 (1.03–61)	0.046

TMD, transmembrane domain; LUAD, lung adenocarcinoma; LUSC, lung squamous carcinoma; HR, hazard ratio.

median OS was 10.0 months (95% CI, 5.0–NA) for *HER2* TMD-mutant patients, and 61.6 months (95% CI, 30.1–NA) for patients harboring non-TMD *HER2* mutations. *Table 2* presents the hazard ratios (HR) associated with clinical and genetic characteristics. OS was significantly worse for *HER2* TMD-mutant patients than non-TMD-mutant patients (HR =7.9, 95% CI: 1.0–61.0, P=0.046). Stage was associated with survival but was not statistically significant in Cox multivariate survival analysis (P=0.47).

Most of the *HER2* TMD-mutant patients (7/8, 87.50%) received more than one line of treatment (*Figure 2B*) and all patients received chemotherapy or combination therapy including chemotherapy as their first-line treatment. Among treatment lines that used only chemotherapy or concurrent chemoradiotherapy, only two lines of treatment in two patients achieved partial response (ORR 22.2%, 2/9). Five patients received targeted therapy as at least one line of therapy and four of these achieved longer OS than the others. However, the choice of targeted therapy was not quite standard. Two patients received EGFR-TKI gefitinib, which was not guideline-recommended, and did not respond (*Figure 2C*). One patient received anti-angiogenesis agent bevacizumab, albeit for only one month before disease progession (*Figure 2C*). The overall response rate (ORR) of targeted therapy in assessable treatment lines was 57.1% (4/7). The longest progression-free survival (PFS) was 16 months, which was achieved by targeted therapy (afatinib) in P12 (*Figure 2D*). However, afatinib was also the most intolerable treatment, and two patients stopped using it because of severe oral ulcers, diarrhea, vomiting, or rash. Four patients received immunotherapy alone as a line of therapy and none of these achieved partial relief during or after the treatment (ORR 0.0%).

A case report of a patient who is responding to pyrotinib as a fifth-line therapy

Patient 01, a 50-year-old Chinese woman with no smoking history, was diagnosed with stage IVa (pT2bN3M1a) LUAD with a rare *HER2* V659E mutation (*Figure 3*). PET-CT revealed a 4.5 cm × 5.3 cm × 3.4 cm mass in the right lower lobe, small, scattered nodules in the left lung, lymph node metastases, and a large amount of malignant pleural effusion. She was treated with lapatinib (1,250 mg, once daily) and capecitabine (2,000 mg, divided into twice daily) as first-line therapy, achieving a partial response (PR) with a PFS of 3 months, after which she presented with fast progression in her primary tumor and chest wall metastasis. Subsequently, afatinib (40 mg daily) was administered as second-line therapy and achieved PR with a PFS of 5 months. At progression, her bone and subcutaneous metastases developed, and subcutaneous tumor tissue samples were sent for NGS testing revealing novel amplifications in both *HER2* and *CCNE1*. Her treatment was then switched to TDM-1 (150 mg daily) and her pain was quickly relieved, but she rapidly progressed to atelectasis and hemoptysis and was subsequently administered with pembrolizumab (90 mg every 3 weeks). While her hemoptysis and pain were significantly alleviated in a week, despite a low tumor mutation burden (TMB), CT showed inflammation and no improvement in the primary nor the metastasized nodules in the lungs and new lesions were seen in the liver, adrenal gland, and abdominal wall. She then received a novel dual EGFR/HER2 inhibitor, pyrotinib, achieving fast reduction of ascites and pain relief and her primary tumor

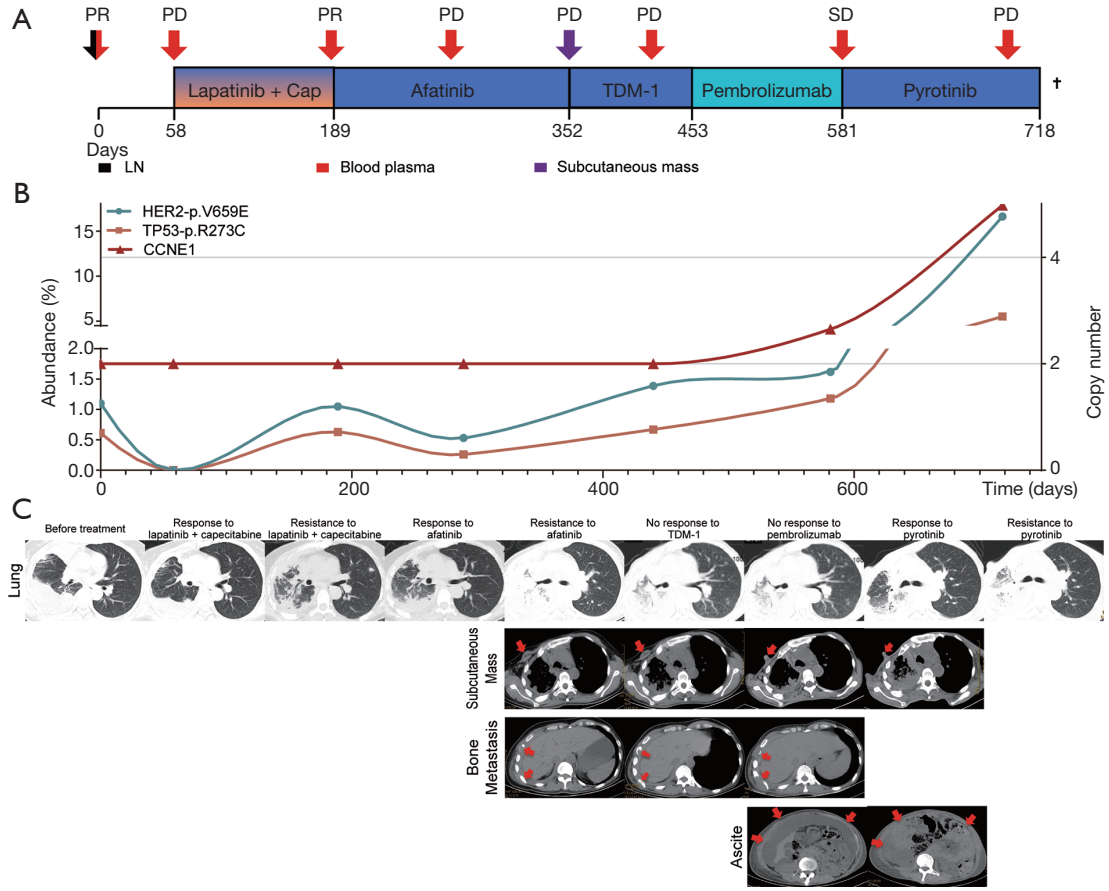

Figure 3 Genomic profiling and treatment regimen of Patient 01 and Docking simulation of *HER2* tyrosine kinase inhibitor. (A) Treatment regimen of patient 01, the duration of each treatment, and the abundance of mutation detected in lymph nodes (LN), pleural effusion, subcutaneous mass, and ascites by next generation sequencing under the various treatments. (B) The dynamic change in circulating tumor DNA (ctDNA) abundance demonstrating the evolution of the patient's tumor. (C) Computed tomography images of the patient's primary lung cancer, metastatic lung, subcutaneous mass, bone disease, and ascites before and after treatments. Subcutaneous mass and bone metastasis developed during progression disease when the patient was taking afatinib and cancerous ascites developed during disease progression when the patient was taking pembrolizumab (lapatinib, 1,250 mg oral daily; capecitabine, 2,000 mg oral divided into twice daily; afatinib, 40 mg oral daily; TDM-1, 150 mg oral daily; pembrolizumab, 100 mg i.v. every 3 weeks; pyrotinib, 400 mg oral daily). The red arrows show subcutaneous metastasis, liver metastasis, and ascites. (A, B, C are accordant in time on the x axis). TMD, transmembrane domain.

and metastatic tumors in the lungs and adrenal gland shrank. Metastatic lesions of the chest wall, bones, subcutaneous tissue, liver, and abdominal wall were also stable. After 3 months of PR, a fast progression in the lung was observed accompanied by the development of ascites and a significant increase in circulating tumor DNA (ctDNA) mutation abundance. The patient passed away shortly after.

Structure and energy analysis of lapatinib, afatinib, and pyrotinib in HER2 kinase domain binding

Lapatinib is a non-covalent inhibitor that interacts with HER2 dynamically as Eq. [1], and afatinib and pyrotinib are covalent inhibitors whose HER2-interaction follows Eq. [2] (E = target, I = inhibitor, [EI] = non-covalent binding state of the target and the inhibitor, EI* = covalently bonded state of the target and the inhibitor). Thus, afatinib and pyrotinib are more favorable for blocking HER2 KD from being continuously phosphorylated than lapatinib. Between the two covalent inhibitors, pyrotinib ($\Delta G_{Pyrotinib}$ = −65.92 kcal/mol) shows stronger non-covalent binding ability than afatinib ($\Delta G_{Afatinib}$ = −59.71 kcal/mol). ΔG calculations of the three TKIs are shown in Table S5 and docking simulation is shown in *Figure 4A,B,C*.

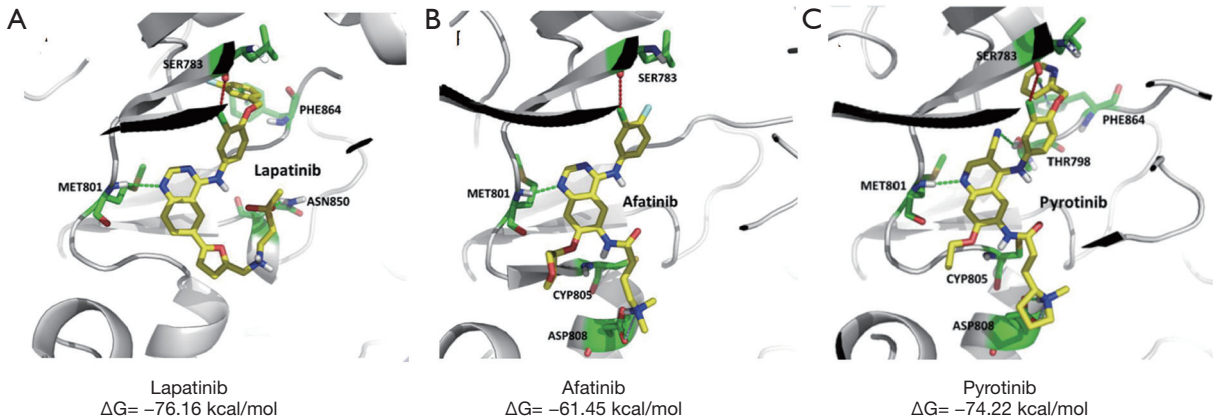

Figure 4 Docking simulation of lapatinib, afatinib, and pyrotinib in the *HER2* kinase domain. The ATP-binding pocket of the *HER2* kinase domain in the modeled *HER2*-lapatinib (A)/afatinib (B)/pyrotinib (C) complex structure is depicted. Lapatinib, afatinib, and pyrotinib are shown as a stick and the structure of the *HER2* kinase domain is shown in tertiary structure. The binding free energy of lapatinib, afatinib, and pyrotinib is shown in the figure.

$$E + I \underset{k_{-1}}{\overset{k_1}{\rightleftharpoons}} [EI] \quad [2]$$

$$E + I \underset{k_{-1}}{\overset{k_1}{\rightleftharpoons}} [EI] \overset{k_{inact}}{\rightarrow} EI^* \quad [3]$$

Discussion

In this study, the incidence of *HER2* TMD mutation was 0.18% (14/7,812) in the Chinese LUAD population. These TMD mutations were more frequent in NSCLC than other solid tumors, and with a higher prevalence in LUAD than lung squamous cell carcinoma (LUSC) (42,56). V659E was the most recurrent mutation compared to that found in colorectal cancer, which was I655V (57). The prevalence of V659E was 0.14% (11/7,812), higher than the mutation rate in the external cohort derived from the TCGA database and ten other studies through cBioPortal (0.10%, 3/2,966) (27-37). The prevalence was also higher than 0.009%, which was reported by Ou *et al.* in 2017 (15). This variation might be explained by differences in the size or race of the investigated cohort. In addition to our current knowledge of all *HER2* KD mutations in published studies that occurred in LUAD (8), all TMD mutations identified in our study also were detected in LUAD and all the *HER2* V659E mutations in our cohort resulted from a dinucleotide missense mutation. It was reported that *HER2* mutation occurred more frequently in younger women and non-smokers (6,8,11,58-60), and rarely co-existed with other lung cancer driver mutations (61). However, we observed no significant difference in gender or smoking history. We also found two patients harboring both *HER2* mutation and *EGFR* or *BRAF* mutations, respectively. This accorded with a previous study that non-KD mutations did not exclude concurrent driver mutations as KD mutations did (8).

Previous studies had reported a shorter OS in *HER2*-mutant lung cancer, especially KD mutations (8,12). The present study found that patients harboring TMD mutations had even shorter OS compared to *HER2* non-TMD mutations with statistical significance (HR 7.9, 95% CI, 1.03–61, P<0.001), including KD mutations. It was also observed that patients harboring TMD mutations were diagnosed at a more advanced stage (HR 1.2, 95% CI, 0.61–2.5, P<0.001), but were not significantly associated with a poorer prognosis.

In the present real-world retrospective cohort, although all patients had the same somatic gene mutation and similar clinical characteristics, their treatment regimens were diverse. For targeted therapy in *HER2* exon 20 insertion, *in vitro* cell-line study demonstrated that the most common YVMA insertion is sensitive to only neratinib, poziotinib, and pyrotinib (24,25). In the clinical setting, targeted therapy is the National Comprehensive Cancer Network (NCCN) guideline-recommended treatment for *HER2* mutation (4). The NCCN recommendation has evolved over time with trastuzumab, lapatinib, and pertuzumab being

recommended in 2013; trastuzumab and afatinib in 2014; and TDM-1 in 2018. However, the works cited to support these recommendations did not include patients harboring *HER2* TMD mutation until Li *et al.* published the results of their basket trial of *HER2*-mutant lung cancers (9). In that study, two V659E patients were recruited in the 18-patient cohort and only one of them achieved PR, while the disease progressed in the other (ORR 50%). In the present cohort, most of the patients received targeted therapies (ORR 57.1%), among which afatinib achieved the longest PFS of 16 months. However, two patients showed intolerance to afatinib and needed an appropriate substitution. Among patients who received targeted therapy, two patients progressed after receiving gefitinib. This suggested *HER2* V659E mutation did not respond to gefitinib, as was demonstrated previously *in vitro* (62). Three patients received immunotherapy, none of whom responded. Although it was previously reported that the response rate to anti-PD-1 immunotherapy in *HER2*-altered NSCLC was 7–35% (63-65), and was similarly low in other driver mutations, a larger cohort is needed to accurately determine the response rate of immunotherapy in *HER2* TMD-mutant patients. Chemotherapy and concurrent chemoradiotherapy were used in all patients (ORR 22.2%), and the efficacy was seen to be better than immunotherapy, although worse than targeted therapy.

We suggest the use of targeted therapy to rechallenge targeted therapy resistance. Previous studies reported short PFS in *HER2* TMD-mutant patients who responded to targeted therapies. The median PFS was 5 months in a basket trial treating *HER2*-mutant NSCLC patients with TDM-1 (9) and PFS was reported to be in the range of 3–18 months (median 5 months) in case reports of patients with *HER2* TMD-mutant patients treated with TKI (15,26,42). As we reported, a stage IV patient with multiple distal metastases achieved an OS of 22.4 months and obtained PR when receiving with first-line lapatinib with capecitabine, second-line afatinib, and fifth-line pyrotinib treatment. Each line of treatment had a PFS longer than 3 months. This might be a solution to conquer the short PFS of targeted therapy. We postulated that pyrotinib can conquer resistance to afatinib, and afatinib to lapatinib because of increased TKI binding affinity. Molecular dynamics simulation and binding free energy analysis were conducted to investigate the binding mode and strength of lapatinib, afatinib, and pyrotinib for the HER2 kinase domain to further explain the sequential conquer of drug resistance in the reported case. The irreversible binding of covalent inhibitors to the target reduces the competition of the endogenous substrate ATP on the kinase, which in turn provides more sustained kinase inhibition than non-covalent inhibitors (66,67). Thus, we conclude that the affinity of lapatinib, afatinib, and pyrotinib increases sequentially.

The efficacy of pyrotinib for tumors harboring an activating *HER2* alteration is being studied in a phase I basket trial including NSCLC (68). Another study reported that LUADs harboring *HER2* KD mutations could respond to pyrotinib better than afatinib (69). The results of our study suggest pyrotinib is also effective for advanced stage *HER2* V659E-mutant LUAD. More refined stratification of patients based on the type of *HER2* activating alterations might be needed in further studies of pyrotinib.

A limitation of this study is that it was a descriptive study based on a real-world multicenter retrospective cohort. The efficacy of targeted therapy, chemotherapy, and immunotherapy should not be directly compared. This limitation reflects the real-world challenge in assembling cohorts of *HER2* TMD-mutant patients because of the low prevalence. While basket trials might serve as a solution, the intra-cohort heterogeneity of prognosis might reduce its reliability in specific mutation subgroups. We suggest finer stratification and transparent data sharing policy in further studies to facilitate future meta-analysis of individual participant data, which is considered as the most accessible high-level evidence for low prevalence mutations.

Conclusions

The present study was the first to report the comprehensive profiles and real-world evidence of treatment responses in *HER2* TMD-mutant lung cancer patients and to report a case that rechallenged TKI resistance with stronger-affinity TKI and responsed to fifth-line pyrotinib.

With the wide application of NGS in tumor evaluation and the inclusion of *HER2* in most NGS panels, more patients with *HER2* TMD mutations have been uncovered. As we have illustrated, patients harboring *HER2* TMD mutations have poorer survival than patients with other *HER2* mutations, highlighting the need for finer stratification of *HER2* mutations in future clinical studies.

Acknowledgments

We thank Ms. Huihui Xu from Nanopep Biotech Co., Beijing, China for her help in organizing materials.

Funding: This work was supported by the National Key Research and Development Program of China (No.

2016YFC0901500), Beijing Health Promotion Association (BJHPA-FW-XHKT-2020040400344), CAMS Innovation Fund for Medical Sciences (2020-I2M-C&T-A-003), Chinese Society of Clinical Oncology CSCO-MSD (Y-MSD2020-0270), Ministry of Science and Technology of the People's Republic of China, Special Data Service for Oncology: The National Population and Health Scientific Data Sharing Platform (NCMI-ABD02-201809 and NCMI-YF02N-201906), and Wu Jieping Medical Foundation Precision Treatment for Thoracic and Abdominal Cancer Fund (320.6750.19092-43).

Footnote

Reporting Checklist: The authors have completed the MDAR reporting checklist. Available at http://dx.doi.org/10.21037/tlcr-21-107

Data Sharing Statement: Available at http://dx.doi.org/10.21037/tlcr-21-107

Conflicts of Interest: All authors have completed the ICMJE uniform disclosure form (available at http://dx.doi.org/10.21037/tlcr-21-107). Dr. JY, Dr. BL, Dr. HHZ, and Dr. JZ report personal fees from Burning Rock Biotechnology Co. Ltd. during the conduct of the study. Dr. NXL reports grants from National Key Research and Development Program of China, Beijing Health Promotion Association, grants from Beijing Natural Science Foundation, Major projects of the Beijing Municipal Science and Technology Commission, and Beijing Dongcheng District Science and Technology Commission Excellent Talents Project, during the conduct of the study. The other authors have no conflicts of interest to declare.

Ethical Statement: The authors are accountable for all aspects of the work in ensuring that questions related to the accuracy or integrity of any part of the work are appropriately investigated and resolved. All procedures performed in studies involving human participants were in accordance with the Helsinki Declaration (as revised in 2013). The study was conducted under the approval of the Ethics Committee of Peking Union Medical College Hospital (ZS-1329). Written informed consent was obtained from each patient.

References

1. Reck M, Rabe KF. Precision Diagnosis and Treatment for Advanced Non–Small-Cell Lung Cancer. N Engl J Med 2017;377:849-61.
2. Nangalia J, Campbell PJ. Genome Sequencing during a Patient's Journey through Cancer. N Engl J Med 2019;381:2145-56.
3. Kobayashi S, Boggon TJ, Dayaram T, et al. EGFR Mutation and Resistance of Non–Small-Cell Lung Cancer to Gefitinib. N Engl J Med 2005;352:786-92.
4. NCCN. Non-Small Cell Lung Cancer (Version 1.2021). National Comprehensive Cancer Network. Available online: https://www.nccn.org/professionals/physician_gls/pdf/nscl.pdf. Accessed 15 Dec 2020.
5. Stephens P, Hunter C, Bignell G, et al. Intragenic ERBB2 kinase mutations in tumours. Nature 2004;431:525-6.
6. Shigematsu H, Takahashi T, Nomura M, et al. Somatic mutations of the HER2 kinase domain in lung adenocarcinomas. Cancer Res 2005;65:1642-6.
7. Pellegrini C, Falleni M, Marchetti A, et al. HER- 2/Neu alterations in non-small cell lung cancer: a comprehensive evaluation by real time reverse transcription-PCR, fluorescence in situ hybridization, and immunohistochemistry. Clin Cancer Res 2003;9:3645-52.
8. Wei XW, Gao X, Zhang XC, et al. Mutational landscape and characteristics of ERBB2 in non-small cell lung cancer. Thoracic Cancer 2020;11:1512-21.
9. Li BT, Shen R, Buonocore D, et al. Ado-Trastuzumab Emtansine for Patients With HER2-Mutant Lung Cancers: Results From a Phase II Basket Trial. J Clin Oncol 2018;36:2532-7.
10. Pillai RN, Behera M, Berry LD, et al. HER2 mutations in lung adenocarcinomas: A report from the Lung Cancer Mutation Consortium. Cancer 2017;123:4099-105.
11. Mazieres J, Peters S, Lepage B, et al. Lung cancer that harbors an HER2 mutation: epidemiologic characteristics and therapeutic perspectives. J Clin Oncol 2013;31:1997-2003.
12. Tomizawa K, Suda K, Onozato R, et al. Prognostic and predictive implications of HER2/ERBB2/neu gene

mutations in lung cancers. Lung Cancer 2011;74:139-44.
13. Kris MG, Johnson BE, Berry LD, et al. Using Multiplexed Assays of Oncogenic Drivers in Lung Cancers to Select Targeted Drugs. JAMA 2014;311:1998.
14. Mineev KS, Bocharov EV, Pustovalova YE, et al. Spatial structure of the transmembrane domain heterodimer of ErbB1 and ErbB2 receptor tyrosine kinases. J Mol Biol 2010;400:231-43.
15. Ou SI, Schrock AB, Bocharov EV, et al. HER2 Transmembrane Domain (TMD) Mutations (V659/G660) That Stabilize Homo- and Heterodimerization Are Rare Oncogenic Drivers in Lung Adenocarcinoma That Respond to Afatinib. J Thorac Oncol 2017;12:446-57.
16. Ma F, Zhang M, Ouyang Q, et al. ERBB2 mutation profiling with next-generation sequencing (NGS) in solid tumors. American Society of Clinical Oncology; 2018.
17. Yu R, Yang SW, Bao H, et al. P2.13-46 Comprehensive Investigation of ERBB2 Transmembrane Domain Mutations (V659/G660) in 12,833 Chinese Lung Cancer Patients. Journal of Thoracic Oncology 2018;13:S816-S7.
18. Xie F, Zhang Y, Mao X, et al. Comparison of genetic profiles among primary lung tumor, metastatic lymph nodes and circulating tumor DNA in treatment-naïve advanced non-squamous non-small cell lung cancer patients. Lung Cancer 2018;121:54-60.
19. Ou S-HI, Madison R, Robichaux JP, et al. Characterization of 648 non-small cell lung cancer (NSCLC) cases with 28 unique HER2 exon 20 insertions. J Clin Oncol 2019;37:9063.
20. Burke CL, Stern DF. Activation of Neu (ErbB-2) mediated by disulfide bond-induced dimerization reveals a receptor tyrosine kinase dimer interface. Mol Cell Biol 1998;18:5371-9.
21. He L, Hristova K. Pathogenic Activation of Receptor Tyrosine Kinases in Mammalian Membranes. J Mol Biol 2008;384:1130-42.
22. Yamamoto H, Higasa K, Sakaguchi M, et al. Novel Germline Mutation in the Transmembrane Domain of HER2 in Familial Lung Adenocarcinomas. JNCI: Journal of the National Cancer Institute 2014;106:djt338.
23. Wang R, Zhang Y, Pan Y, et al. Comprehensive investigation of oncogenic driver mutations in Chinese non-small cell lung cancer patients. Oncotarget 2015;6:34300.
24. Oh DY, Bang YJ. HER2-targeted therapies — a role beyond breast cancer. Nat Rev Clin Oncol 2020;17:33-48.
25. Baraibar I, Mezquita L, Gil-Bazo I, et al. Novel drugs targeting EGFR and HER2 exon 20 mutations in metastatic NSCLC. Crit Rev Oncol Hematol 2020;148:102906.
26. Serra V, Vivancos A, Puente XS, et al. Clinical response to a lapatinib-based therapy for a Li-Fraumeni syndrome patient with a novel HER2V659E mutation. Cancer Discov 2013;3:1238-44.
27. Ding L, Getz G, Wheeler DA, et al. Somatic mutations affect key pathways in lung adenocarcinoma. Nature 2008;455:1069-75.
28. Imielinski M, Berger AH, Hammerman PS, et al. Mapping the hallmarks of lung adenocarcinoma with massively parallel sequencing. Cell 2012;150:1107-20.
29. Rizvi NA, Hellmann MD, Snyder A, et al. Cancer immunology. Mutational landscape determines sensitivity to PD-1 blockade in non-small cell lung cancer. Science 2015;348:124-8.
30. Campbell JD, Alexandrov A, Kim J, et al. Distinct patterns of somatic genome alterations in lung adenocarcinomas and squamous cell carcinomas. Nat Genet 2016;48:607-16.
31. Abbosh C, Birkbak NJ, Wilson GA, et al. Phylogenetic ctDNA analysis depicts early-stage lung cancer evolution. Nature 2017;545:446-51.
32. Jamal-Hanjani M, Wilson GA, McGranahan N, et al. Tracking the Evolution of Non-Small-Cell Lung Cancer. N Engl J Med 2017;376:2109-21.
33. Jordan EJ, Kim HR, Arcila ME, et al. Prospective Comprehensive Molecular Characterization of Lung Adenocarcinomas for Efficient Patient Matching to Approved and Emerging Therapies. Cancer Discov 2017;7:596-609.
34. Vavalà T, Monica V, Lo Iacono M, et al. Precision medicine in age-specific non-small-cell-lung-cancer patients: Integrating biomolecular results into clinical practice-A new approach to improve personalized translational research. Lung Cancer 2017;107:84-90.
35. Hellmann MD, Nathanson T, Rizvi H, et al. Genomic Features of Response to Combination Immunotherapy in Patients with Advanced Non-Small-Cell Lung Cancer. Cancer Cell 2018;33:843-52.e4.
36. Rizvi H, Sanchez-Vega F, La K, et al. Molecular Determinants of Response to Anti-Programmed Cell Death (PD)-1 and Anti-Programmed Death-Ligand 1 (PD-L1) Blockade in Patients With Non-Small-Cell Lung Cancer Profiled With Targeted Next-Generation Sequencing. J Clin Oncol 2018;36:633-41.
37. Chen J, Yang H, Teo ASM, et al. Genomic landscape of lung adenocarcinoma in East Asians. Nat Genet 2020;52:177-86.

38. Cerami E, Gao J, Dogrusoz U, et al. The cBio Cancer Genomics Portal: An Open Platform for Exploring Multidimensional Cancer Genomics Data: Figure 1. Cancer Discovery 2012;2:401-4.
39. Gao J, Aksoy BA, Dogrusoz U, et al. Integrative analysis of complex cancer genomics and clinical profiles using the cBioPortal. Sci Signal 2013;6:pl1.
40. Wang Z, Yang JJ, Huang J, et al. Lung Adenocarcinoma Harboring EGFR T790M and In Trans C797S Responds to Combination Therapy of First- and Third-Generation EGFR TKIs and Shifts Allelic Configuration at Resistance. J Thorac Oncol 2017;12:1723-7.
41. Sun Y, Ren Y, Fang Z, et al. Lung adenocarcinoma from East Asian never-smokers is a disease largely defined by targetable oncogenic mutant kinases. J Clin Oncol 2010;28:4616-20.
42. Pahuja KB, Nguyen TT, Jaiswal BS, et al. Actionable Activating Oncogenic ERBB2/HER2 Transmembrane and Juxtamembrane Domain Mutations. Cancer Cell 2018;34:792-806 e5.
43. Morris GM, Huey R, Lindstrom W, et al. AutoDock4 and AutoDockTools4: Automated docking with selective receptor flexibility. J Comput Chem 2009;30:2785-91.
44. Fuhrmann J, Rurainski A, Lenhof HP, et al. A new Lamarckian genetic algorithm for flexible ligand-receptor docking. J Comput Chem 2010;31:1911-8.
45. Case DA, Cheatham TE, 3rd, Darden T, et al. The Amber biomolecular simulation programs. J Comput Chem 2005;26:1668-88.
46. Duan Y, Wu C, Chowdhury S, et al. A Point-Charge Force Field for Molecular Mechanics Simulations of Proteins Based on Condensed-Phase Quantum Mechanical Calculations. J Comput Chem 2003;24:1999-2012.
47. Wang J, Wolf RM, Caldwell JW, et al. Development and Testing of a General Amber Force Field. J Comput Chem 2004;25:1157-74.
48. Jakalian A, Bush BL, Jack DB, et al. Fast, Efficient Generation of High-Quality Atomic Charges. AM1-BCC Model: I. Method. J Comput Chem 2000;21:132-46.
49. Jakalian A, Jack DB, Bayly CI. Fast, efficient generation of high-quality atomic charges. AM1-BCC model: II. Parameterization and validation. J Comput Chem 2002;23:1623-41.
50. Wang J, Wang W, Kollman PA, et al. Automatic atom type and bond type perception in molecular mechanical calculations. J Mol Graph Model 2006;25:247-60.
51. Jorgensen WL, Chandrasekhar J, Madura JD, et al. Comparison of simple potential functions for simulating liquid water. The Journal of Chemical Physics 1983;79:926-35.
52. Kollman PA, Massova I, Reyes C, et al. Calculating Structures and Free Energies of Complex Molecules: Combining Molecular Mechanics and Continuum Models. Acc Chem Res 2000;33:889-97.
53. Miller BR, McGee TD, Swails JM, et al. MMPBSA.py: An Efficient Program for End-State Free Energy Calculations. J Chem Theory Comput 2012;8:3314-21.
54. Wilkinson L. ggplot2: elegant graphics for data analysis by WICKHAM, H. Biometrics 2011;67:678-9.
55. Therneau TM. A Package for Survival Analysis in R. R package version 3.2-7 ed2020.
56. Ross JS, Fakih M, Ali SM, et al. Targeting HER2 in colorectal cancer: The landscape of amplification and short variant mutations in ERBB2 and ERBB3. Cancer 2018;124:1358-73.
57. Loree JM, Bailey AM, Johnson AM, et al. Molecular Landscape ofERBB2/ERBB3Mutated Colorectal Cancer. J Natl Cancer Inst 2018;110:1409-17.
58. Mazieres J, Barlesi F, Filleron T, et al. Lung cancer patients with HER2 mutations treated with chemotherapy and HER2-targeted drugs: results from the European EUHER2 cohort. Ann Oncol 2016;27:281-6.
59. Chuang JC, Stehr H, Liang Y, et al. ERBB2-Mutated Metastatic Non-Small Cell Lung Cancer: Response and Resistance to Targeted Therapies. J Thorac Oncol 2017;12:833-42.
60. Arcila ME, Chaft JE, Nafa K, et al. Prevalence, clinicopathologic associations, and molecular spectrum of ERBB2 (HER2) tyrosine kinase mutations in lung adenocarcinomas. Clin Cancer Res 2012;18:4910-8.
61. Ricciardi GR, Russo A, Franchina T, et al. NSCLC and HER2: between lights and shadows. J Thorac Oncol 2014;9:1750-62.
62. Suzawa K, Toyooka S, Sakaguchi M, et al. Antitumor effect of afatinib, as a human epidermal growth factor receptor 2-targeted therapy, in lung cancers harboring HER2 oncogene alterations. Cancer Sci 2016;107:45-52.
63. Lai W-CV, Feldman DL, Buonocore DJ, et al. PD-L1 expression, tumor mutation burden and response to immune checkpoint blockade in patients with HER2-mutant lung cancers. J Clin Oncol 2018;36:9060.
64. Mazieres J, Drilon A, Lusque A, et al. Immune checkpoint inhibitors for patients with advanced lung cancer and oncogenic driver alterations: results from the IMMUNOTARGET registry. Ann Oncol 2019;30:1321-8.

65. Guisier F, Dubos-Arvis C, Viñas F, et al. Efficacy and Safety of Anti-PD-1 Immunotherapy in Patients With Advanced NSCLC With BRAF, HER2, or MET Mutations or RET Translocation: GFPC 01-2018. J Thorac Oncol 2020;15:628-36.
66. Barf T, Kaptein A. Irreversible Protein Kinase Inhibitors: Balancing the Benefits and Risks. J Med Chem 2012;55:6243-62.
67. Bauer RA. Covalent inhibitors in drug discovery: from accidental discoveries to avoided liabilities and designed therapies. Drug Discovery Today 2015;20:1061-73.
68. Li BT, Li T, Johnson ML, et al. Safety and efficacy of pyrotinib in patients with NSCLC and other advanced solid tumors with activating HER2 alterations: A phase I basket trial. J Clin Oncol 2020;38:3510.
69. Wang Y, Jiang T, Qin Z, et al. HER2 exon 20 insertions in non-small-cell lung cancer are sensitive to the irreversible pan-HER receptor tyrosine kinase inhibitor pyrotinib. Ann Oncol 2019;30:447-55.

(English Language Editor: B. Draper)

Cite this article as: Jia Z, Xing J, Li J, Wang W, Wang Y, Song Y, Yang X, Xue J, Ye J, Li B, Han-Zhang H, Zhao J, Zhang X, Peng F, Chen F, Chen X, Lu Y, Ying S, Wu D, Zhang X, Ma C, Lai L, Ma S, Liang D, Liu P, Li X, Liang N, Li S. *HER2* transmembrane domain mutation: comprehensive characteristics and real-world evidence of treatment response in Chinese lung adenocarcinoma. Transl Lung Cancer Res 2021;10(3):1383-1396. doi: 10.21037/tlcr-21-107

Table S1 The 520 cancer-related genes included in the OncoScreen Plus panel

ABL1	CDK4	ESR2	ICOSLG	MSH6	POLE	SMO
ABL2	CDK6	EWSR1	ID3	MST1	POM121L12	SNCAIP
ACVR1	CDK8	EZH2	IDH1	MST1R	PPM1D	SOCS1
ACVR1B	CDKN1A	FAM175A	IDH2	MTOR	PPP2R1A	SOX2
ADGRA2	CDKN1B	FAM46C	IFNGR1	MUTYH	PPP2R2A	SOX9
AKT1	CDKN1C	FANCA	IGF1	MYC	PPP6C	SOX10
AKT2	CDKN2A	FANCC	IGF1R	MYCL	PRDM1	SOX17
AKT3	CDKN2B	FANCD2	IGF2	MYCN	PREX2	SPEN
ALK	CDKN2C	FANCE	IKBKE	MYD88	PRKAR1A	SPOP
ALOX12B	CEBPA	FANCF	IKZF1	MYOD1	PRKC1	SPTA1
AMER1	CENPA	FANCG	IL10	NBN	PRKDC	SRC
ANKRD11	CHD1	FANCI	IL7R	NCOA3	PRSS8	SRSF2
APC	CHD2	FANCL	INHA	NCOR1	PTCH1	STAG2
APCDD1	CHD4	FANCM	INHBA	NEB	PTEN	STAT3
AR	CHEK1	FAS	INPP4A	NEGR1	PTK2	STAT4
ARAF	CHEK2	FAT1	INPP4B	NF1	PTPN11	STAT5A
ARFRP1	CHUK	FAT3	INSR	NF2	PTPRD	STAT5B
ARID1A	CIC	FBXW7	IRF2	NFE2L2	PTPRS	STK11
ARID1B	CRBN	FCGR2B	IRF4	NFKB1A	PTPRT	STK40
ARID2	CREBBP	FGF10	IRS1	NKX2-1	QK1	SUFU
ARID5B	CRKL	FGF12	IRS2	NKX3-1	RAB35	SUZ12
ASXL1	CRLF2	FGF23	JAK1	NOTCH1	RAC1	SYK
ASXL2	CSF1R	FGF6	JAK2	NOTCH2	RAD21	TACC3
ATF1	CSF3R	FGF7	JAK3	NOTCH3	RAD50	TAF1
ATM	CTCF	FGFR14	JUN	NOTCH4	RAD51	TBX3
ATR	CTLA4	FGFR1	KAT5A	NPM1	RAD51B	TCF3
ATRX	CTNNA1	FGFR2	KDM5A	NRAS	RAD51C	TCF7L2
AURKA	CTNNB1	FGFR3	KDM5C	NR4A3	RAD51D	TERC
AURKB	CUL3	FOXA1	KDM6A	NRG1	RAD52	TERT
AXIN1	CUL4A	FOXL2	KDR	NSD1	RAD54L	TET1
AXIN2	CUL4B	FRS2	KEAP1	NTHL1	RAF1	TET2
AXL	CXCR4	FYN	KEL	NTRK1	RANBP2	TGFBR1
B2M	CYCLD	GABRA6	KIT	NTRK2	RARA	TGFBR2
BACH1	CYP17A1	GATA4	KLF4	NTRK3	RASA1	TIPARP
BAP1	DAXX	GATA6	KLHL6	NUP93	RB1	TMEM127
BARD1	DCUN1D1	GID4	KMT2A	PAK1	RBM10	TMPR552
BBC3	DDR2	GNA13	KMT2C	PAK3	RECQL4	TNFAIP3
BCL2	DICER1	GPS2	KMT2D	PAK7	REL	TNFRSF14
BCL10	DIS3	GREM1	KRAS	PALB2	RET	TNFSF11
BCL2L1	DNAJB1	GRM3	LATS1	PARK2	RFWD2	TOP1
BCL2L11	DNMT1	GSK3B	LATS2	PARP1	RHEB	TOP2A
BCL2L2	DNMT3A	GSTM1	LMO1	PARP2	RHOA	TP53
BCL6	DNMT3B	GSTT1	LRP1B	PARP3	RICTOR	TRAF2
BCOR	DOT1L	H3F3A	LYN	PARP4	RIT1	TRAF7
BCORL1	E2F3	H3F3B	LZTR1	PAX5	RNF43	TRRAP
BCR	EED	HDAC1	MAG12	PBRM1	ROS1	TSC1
BLM	EGFL7	HDAC2	MALT1	PDCD1	RPA1	TSC2
BMPR1A	EGFR	HDAC4	MAP2K1	PDCD1LG2	RPS6KA4	TSHR
BRAF	EIF1AX	HGF	MAP2K2	PDFRA	RPS6KB2	U2AF1
BRCA1	EIF4A2	HIST1H1C	MAP2K4	PDGFRB	RPTOR	VEGFA
BRCA2	EIF4E	HIST1H2BD	MAP3K1	PDK1	RUNX1	VEGFB
BRD4	ELOC	HIST1H3A	MAP3K13	PGR	RUNX1T1	VEGFC
BRIP1	EMSY	HIST1H3B	MAP3K14	PHOX2B	RYBP	VHL
BTG1	EP300	HIST1H3C	MAP3K3	PIK3CA	SDHA	VTCN1
BTK	EPCAM	HIST1H3D	MAPK1	PIK3CB	SDHAF2	WISP3
CALR	EPHA2	HIST1H3E	MAX	PIK3C2B	SDHB	WRN
CARD11	EPHA3	HIST1H3F	MCL1	PIK3C2G	SDHC	WT1
CASP8	EPHA5	HIST1H3G	MDM2	PIK3C3	SDHD	XIAP
CBFB	EPHA7	HIST1H3H	MDM4	PIK3CD	SETD2	XPO1
CBL	EPHB1	HIST1H3I	MED12	PIK3CG	SF3B1	XRCC2
CCND1	ERBB2	HIST1H3J	MEF2B	PIK3R1	SH2B3	XRCC3
CCND2	ERBB3	HIST2H3C	MEN1	PIK3R2	SH2D1A	YAP1
CCND3	ERBB4	HIST2H3D	MET	PIK3R3	SHQ1	YES1
CCNE1	ERBB5	HIST3H3	MGA	PIM1	SLIT2	ZBTB2
CD274	ERCC1	HLA-A	MITF	PLCG2	SLX4	ZFHX3
CD276	ERCC2	HNF1A	MLH1	PLK2	SMAD2	ZNF217
CD79A	ERCC3	HNF1B	MLH3	PMAIP1	SMAD3	ZNF703
CD79B	ERCC4	HOXB13	MPL	PMS1	SMAD4	ZNRF3
CDC73	ERCC5	HRAS	MRE11A	PMS2	SMARCA4	ZRSR2
CDH1	ERG	HSD3B1	MSH2	PNRC1	SMARCB1	
CDK12	ERRFI1	HSP90AA1	MSH3	POLD1	SMARCD1	

http://dx.doi.org/10.21037/tlcr-21-107

Table S2 The 168 cancer-related genes included in the OncoScreen Plus panel

AKT1	CDK6	FAT3	JAK1	NBN	PTPRT	TGFBR2
ALK	CDKN1A	FBXW7	JAK2	NF1	RAD50	TP53
APC	CDKN1B	FGF19	KDM5A	NOTCH1	RAD51B	TP63
AR	CDKN2A	FGF3	KDM6A	NRAS	RAD51C	TRIM58
ARID1A	CHEK1	FGF4	KDR	NRG1	RAD51D	TRPC5
ATM	CHEK2	FGFR1	IGF1	NTRK1	RAD54L	U2AF1
ATR	CREBBP	FGFR2	IGF1R	NTRK2	RAF1	UGT1A1
B2M	CSMD3	FGFR3	KEAP1	NTRK3	RARA	VEGFA
BARD1	CTNNB1	FLT1	KIT	PAK5	RB1	VEGFB
BCL2L11	CYP2A6	FLT3	KMT2D	PALB2	RBM10	VEGFC
BCOR	DIS3	FLT4	KRAS	PARP1	RET	VHL
BLM	DNMT3A	GATA2	LRP1B	PDGFRA	RNF43	YES1
BRAF	DPYD	GATA3	MAP2K1	PDGFRB	ROS1	
BRCA1	EGFR	GRIN2A	MAP3K13	PIK3C2G	RUNX1	
BRCA2	EMSY	H3F3C	MAX	PIK3C3	SETD2	
BRINP3	EP300	HGF	MCL1	PIK3CA	SMAD4	
BRIP1	EPHA3	HIST1H1C	MEN1	PIK3CG	SMARCA4	
CARD11	EPHA5	HIST1H3B	MET	PIK3R1	SOX2	
CASP8	EPHA7	HIST1H3G	MRE11	PMS2	SOX9	
CBL	EPHB1	HRAS	MSH2	POLD1	SPOP	
CCND1	ERBB2	IDH1	MSH6	POLE	SPTA1	
CCNE1	ERBB3	IDH2	MTOR	POM121L12	SRC	
CD274	ERBB4	IGF2	MUTYH	PPP2R1A	STAG2	
CD74	ESR1	IKZF1	MYC	PRKDC	STK11	
CDH18	FANCA	IL7R	MYCN	PTEN	TBX3	
CDK4	FANCI	INHBA	NAV3	PTPRD	TERT	

Table S3 The eight cancer-related genes included in the OncoScreen Plus panel

EGFR
ALK
BRAF
ERBB2
KRAS
MET
RET
ROS1

http://dx.doi.org/10.21037/tlcr-21-107

Table S4 Clinicopathologic features of *HER2* TMD mutation V659E in lung adenocarcinomas

No.	Onset Age, y	Gender	Smoking status	Histologic subtype	Stage	Baseline ECOG-PS	TMD Protein Alteration	ERBB2/*HER2* alteration	Abundance
1	48	F	Positive history	Adenocarcinoma	IVa	1	V659E	c.1976_1977delTTinsAA	32.50%
2	68	M	Never-smoker	Adenocarcinoma+Neuroendocrinal differenciation	IVa	1	V659E	c.1976_1977inv	1.84%
3	53	M	Never-smoker	Adenocarcinoma	IVa	NR	V659E	c.1976_1978inv	86.90%
4	69	F	Positive history	Adenocarcinoma	IVc	1	V659E	c.1976_1979inv	17.20%
5	60	M	Never-smoker	Adenocarcinoma	IVc	0	V659E	c.1976_1980inv	22.84%
6	65	F	Positive history	Adenocarcinoma	IVb	2	V659E	c.1976_1977delinsAG	26.54%
7	72	M	Never-smoker	Adenocarcinoma	IVa	1	V659E	c.1976_1977delinsAG	1.16%
8	75	M	Never-smoker	Adenocarcinoma	IVa	NR	V659E	c.1976_1977inv	11.38%
9	75	F	Never-smoker	Adenocarcinoma	IVa	NR	V659E	c.1976_1978inv	41.60%
10	69	M	Never-smoker	Adenocarcinoma	IV	NR	V659E	c.1976_1979inv	28.50%
11	70	M	Positive history	Adenocarcinoma	IA	0	V659E	c.1976_1977delinsAG	11.61%
12	44	F		Adenocarcinoma	NR	NR	V659E	c.1976_1977delinsAG	
13	69	F	Never-smoker	Adenocarcinoma	IA	NR	V659E	c.1976_1977inv	
14	55	F	Never-smoker	Adenocarcinoma	IA	NR	V659E	c.1976_1978inv	
15	45	M	NR	Adenocarcinoma	IVb	NR	V659E	c.1976_1977delinsAG	
16	67	F	NR	Adenocarcinoma	IVa	NR	V659E	c.1976_1977delinsAG	

Table S5 The ΔG value of molecules non-covalent binding with *HER2* kinase.

Ligand	VDWAALS (kcal/mol)	EEL (kcal/mol)	EGB (kcal/mol)	ESURF (kcal/mol)	ΔG (kcal/mol)
Lapatinib	-76.16	17.98	9.91	-8.85	-57.12
Afatinib	-61.45	-65.53	74.82	-7.55	-59.71
Pyrotinib	-74.22	-7.9	25.4	-9.19	-65.92

http://dx.doi.org/10.21037/tlcr-21-107